



## QUANTITATIVE AND MORPHOMETRIC DATA INDICATE PRECISE CELLULAR INTERACTIONS BETWEEN SEROTONIN TERMINALS AND POSTSYNAPTIC TARGETS IN RAT SUBSTANTIA NIGRA

H. MOUKHLES,\* O. BOSLER,† J. P. BOLAM,‡ A. VALLÉE,\* D. UMBRIACO,\*  
 M. GEFFARD§ and G. DOUCET\*||

\*Département de pathologie and Centre de recherche en sciences neurologiques, Faculté de médecine, Université de Montréal, case postale 6128, succursale centre-ville, Montréal, Québec, Canada H3C 3J7

†Institut Fédératif Jean Roche, INSERM, U297, Faculté de médecine Nord, Marseille, France

‡MRC Anatomical Neuropharmacology Unit, Department of Pharmacology, Oxford, U.K.

§Immunopathologie, EPHE-PION-ENSCP, Talence, France

**Abstract**—We have quantified the density of serotonin axonal varicosities, their synaptic incidence and their distribution among potential targets in the pars reticulata and pars compacta of the rat substantia nigra. Serotonin axonal varicosities, counted at the light microscopic level following *in vitro* [<sup>3</sup>H]serotonin uptake and autoradiography, amounted to  $9 \times 10^6/\text{mm}^3$  in the pars reticulata and  $6 \times 10^6/\text{mm}^3$  in the pars compacta, among the densest serotonin innervations in brain. As determined at the electron microscopic level following immunolabelling for serotonin, virtually all serotonin varicosities in the pars reticulata and 50% of those in the pars compacta formed a synapse, essentially with dendrites. The combination of serotonin immunocytochemistry with tyrosine hydroxylase immunolabelling of dopamine neurons reveals that 20% of the serotonin synaptic contacts in the pars reticulata are on dopamine dendrites and 6% are on a type of unlabelled dendrite characterized by its peculiarly high cytoplasmic content of microtubules. The comparison of the diameter of the dendritic profiles that were in synaptic contact with serotonin-immunoreactive varicosities with the diameter of all other dendritic profiles of the same type suggests that serotonergic varicosities innervate dopamine dendrites uniformly along their length, whereas they tend to contact microtubule-filled dendrites in more proximal regions and the other, unidentified dendrites in more distal regions. Furthermore, the size of the serotonin-immunoreactive varicosities and of their synaptic junctions is significantly smaller on dopamine dendrites and larger on microtubule-filled dendrites than on other, unidentified dendrites, indicating that the nature of the postsynaptic target is an important determinant of synaptic dimensions.

These data should help to clarify the role of serotonin in the nigral control of motor functions. They indicate that this dense serotonin input to the substantia nigra is very precisely organized, acting through both “non-junctional” and “junctional” modes of neurotransmission in the pars compacta, which projects to the neostriatum and the limbic system, whereas the predominant mode of serotonin transmission appears to be of the “junctional” type in the pars reticulata, where serotonin can finely control the motor output of the basal ganglia by acting on the GABA projection neurons either directly or through the local release of dopamine by dopaminergic dendrites. The data also raise the possibility that the postsynaptic targets have trophic retrograde influences on serotonergic terminals. Copyright © 1996 IBRO. Published by Elsevier Science Ltd.

**Key words:** serotonin innervation, substantia nigra, dopamine neurons, dark neurons, ultrastructure, cellular interactions.

Brain regions involved in the control of motor functions are currently known to be densely innervated by serotonin (5-HT) fibres, supporting an important role

of 5-HT in the regulation of such functions.<sup>28</sup> In the substantia nigra (SN), whose 5-HT input is topographically organized and originates in the mesencephalic (dorsal and median) raphe nuclei (see Ref. 10), unilateral injection of 5-HT induces a contralateral rotational behaviour, particularly in 5,7-dihydroxytryptamine-lesioned rats,<sup>4,36</sup> supporting a role for nigral 5-HT in motor control. Although this effect might be at least partly independent of dopamine (DA), as assessed following 6-hydroxydopamine destruction of the nigral DA neurons,<sup>36</sup> 5-HT excites these neurons<sup>35</sup> and

||To whom correspondence should be addressed.

**Abbreviations:** ABC, avidin-biotin complex; DA, dopamine; DAB, diaminobenzidine; 5-HT, serotonin (5-hydroxytryptamine); MT, microtubule-filled, electron-dense dendrites; PB, phosphate buffer; SN, substantia nigra; SNc, substantia nigra pars compacta; SNr, substantia nigra pars reticulata; TH, tyrosine hydroxylase; TMBS, Tris-hydrochloride buffer containing sodium metabisulphite.

induces the local dendritic release of DA,<sup>52</sup> possibly through the facilitation of a calcium conductance in DA dendrites.<sup>34</sup> As a morphological support, direct synaptic contacts have indeed been demonstrated between 5-HT-immunoreactive axonal varicosities, or axonal varicosities labelled following tract tracer injections into the dorsal raphe, and nigral DA [tyrosine hydroxylase (TH)-immunostained] dendrites.<sup>10,34</sup> There is, however, no quantitative data on the cellular relationships of these terminals with either their DA targets or other types of nigral neurons. Furthermore, 5-HT varicosities have not been investigated for their synaptic incidence in the SN, as opposed to various other regions of the brain, where they have been reported to mostly lack the junctional specializations typical of synaptic contacts (for review, see Ref. 44).

The present study was undertaken to deepen our understanding of the position occupied by the 5-HT projection in the neural circuitry of the SN by providing quantitative data on the density of this input, on the proportion of 5-HT varicosities involved in morphologically-defined synapses and on their postsynaptic elements. For this purpose, we investigated separately the two parts of the SN, namely its pars compacta (SNc), which includes most of the nigral DA neurons, and its pars reticulata (SNr), which receives dendritic projections from the DA neurons of the ventral tier of the SNc and is populated by the GABA output neurons. The density of 5-HT innervation was quantified on light microscope autoradiographs from the rostral part of the SN following a technique based on *in vitro* uptake of tritiated 5-HT.<sup>17,18</sup> Cellular relationships of the 5-HT varicosities were analysed by electron microscopy following peroxidase pre-embedding immunostaining with a monoclonal antibody recognizing a 5-HT-glutaraldehyde-protein conjugate.<sup>25</sup> Identification of DA postsynaptic targets was carried out following immunostaining for both 5-HT and TH, using a combined peroxidase and silver-immunogold labelling procedure.<sup>8</sup>

## EXPERIMENTAL PROCEDURES

### Materials

The following special chemicals and drugs were used in the present study. Sodium pentobarbital (Somnotol, 70 mg/kg *i.p.*; MTC Pharmaceuticals, Cambridge, On, Canada); glutaraldehyde (EM grade; Mecalab, Montréal, Qc, Canada); osmium tetroxide (Mecalab); epoxy resins (Epon 812; Mecalab or Durcupan ACM; Fluka, Buchs, Switzerland); tritiated serotonin [5-(1,2-<sup>3</sup>H(N))-hydroxytryptamine creatinine sulphate]; NET-498, 1032 GBq/mmol; DuPont-NEN, Boston, MA); pargyline (Aldrich, Milwaukee, WI); benztropine mesylate (Cogentin; Merck, Sharp and Dohme, Kirkland, Qc, Canada); nuclear emulsion (K-5; Ilford, Cheshire, U.K.); a monoclonal antibody against 5-HT-glutaraldehyde-protein conjugate;<sup>25</sup> polyclonal antibodies against TH (Pel-Freez, Rogers, AR); a biotinylated horse anti-mouse antibody (Vector, Burlingame, CA); an avidin-biotin-peroxidase complex (ABC kit, Vectastain; Vector); goat anti-rabbit antibodies

conjugated to 1 nm gold particles (AuroProbe One GAR, 1/50; Amersham, Buckinghamshire, U.K.) and a silver enhancement kit (Intense M, Amersham); pioloform (Polaron, Bio-Rad, Cambridge, MA).

### Animals

The study was performed on 17 adult female Sprague-Dawley rats (225–250 g; Charles River, Montréal, Qc, Canada). All efforts were made to minimize animal suffering and to reduce the number of animals used. These experiments did not involve *in vivo* techniques. The animals were deeply anaesthetized with sodium pentobarbital and perfused through the ascending aorta either with 300 ml ice-cold artificial cerebrospinal fluid (see Ref. 17), for [<sup>3</sup>H]5-HT uptake/storage and autoradiography (*n*=3), or with saline buffered with 0.01 M sodium phosphate (PBS; pH 7.4) followed by 500–700 ml of 3.5% glutaraldehyde prepared in 0.1 M sodium phosphate buffer (PB, pH 7.4) containing 0.2% sodium metabisulphite, for 5-HT and TH immunocytochemistry (*n*=14).

### Quantification of serotonergic terminals

Slices of fresh midbrain tissue from three rats were processed for [<sup>3</sup>H]5-HT uptake/storage and autoradiography in order to quantify the number of 5-HT axonal varicosities/mm<sup>3</sup> of the SNr and SNc according to a procedure described in detail elsewhere.<sup>17,18</sup> Briefly, 200- $\mu$ m-thick slices of the midbrain between planes Bregma -4.8 and -5.6 in the atlas of Paxinos and Watson<sup>39</sup> were incubated with 1  $\mu$ M of [<sup>3</sup>H]5-HT in the presence of pargyline (0.1 mM) and benztropine (1  $\mu$ M). The slices were fixed with glutaraldehyde and with osmium tetroxide vapours and embedded in Epon 812. From each rat, three to four semithin sections (4- $\mu$ m-thick) of the whole midbrain slices were cut on a Polycut<sup>®</sup> microtome (Reichert-Jung; Vienna, Austria) and dipped in liquified nuclear emulsion, which was developed in freshly prepared D-19 after three weeks exposure. Silver grain clusters representing labelled 5-HT axonal varicosities were counted by computerized image analysis (ImageSet; DappleSystems, Sunnyvale, CA). On each section, counting was performed in three regions of the SNr and two regions of the SNc, with a counting window of the size illustrated in Fig. 1. The raw data expressed as number of silver grain clusters/unit area were extrapolated to number/unit volume as described previously.<sup>17,18</sup> For that purpose, a separate series of semithin sections (0.5- $\mu$ m-thick) was dipped in nuclear emulsion and developed after 5–60 days to determine the effect of autoradiographic exposure time on the number of detected 5-HT axonal varicosities.

### Pre-embedding immunocytochemistry

**Single immunolabelling.** 50- $\mu$ m-thick Vibratome sections of the glutaraldehyde-fixed midbrain were rinsed in 0.05 M Tris-HCl buffer containing 0.9% sodium metabisulphite (TMBS; pH 7.4) and incubated in TMBS containing 0.5% sodium borohydride for 5–10 min. They were cryoprotected in TMBS containing 31% sucrose and 13% glycerol (15 min), frozen in liquid nitrogen-cooled isopentane and then in liquid nitrogen (10 s each) and thawed in TMBS. They were immunostained with a primary monoclonal antibody against a 5-HT-glutaraldehyde-protein conjugate (1/5000)<sup>25</sup> following a procedure described elsewhere,<sup>19,32</sup> using a biotinylated horse anti-mouse IgG (1/200) and ABC. The peroxidase activity was revealed with 0.05% 3,3'-diaminobenzidine (DAB; Sigma) and 0.004% hydrogen peroxide.

**Double immunolabelling.** Dual staining for 5-HT and TH was accomplished following the DAB-immunogold method of Chan *et al.*<sup>8</sup> Sections were incubated simultaneously

with a polyclonal antibody against TH (1/500) and the monoclonal antibody against 5-HT-glutaraldehyde-protein conjugate for 48 h. Immunostaining for 5-HT was obtained as above and TH immunoreactivity was revealed by the immunogold procedure, using goat anti-rabbit antibodies conjugated to 1 nm gold particles which were intensified by silver enhancement. Control sections were incubated in parallel, following the same procedure, except that one of the primary antibodies was omitted. These control sections confirmed the specificity of labelling: no DAB-labelled terminals and no immunogold-labelled somata or dendrites were seen when the 5-HT or TH antibody was omitted, respectively. Moreover, previous experiments with the same antibodies, in the same conditions, on sections from 5,7-dihydroxytryptamine- or 6-hydroxydopamine-lesioned rats showed markedly reduced numbers of 5-HT- or TH-immunopositive cell bodies in the dorsal raphe or SN, respectively.<sup>32,33</sup> In these animals, there was also a concomitant reduction of 5-HT- or TH-labelled axonal fibres in the projection areas, e.g., the SN or striatum, respectively. The immunostained sections were post-fixed with 1% osmium tetroxide in 0.1 M PB for 30 min, dehydrated in graded series of dilutions of ethanol and flat-embedded in Durcupan. After re-embedding of selected areas, serial ultrathin sections (silver, 50 nm) from the SNr and SNc were cut on an Ultracut ultramicrotome (Reichert-Jung) and collected on single-slot copper grids coated with pioloform. Sections were counterstained with lead citrate<sup>41</sup> and examined with Philips EM 300G or CM 100 electron microscopes at a working magnification of  $\times 14,500$ .

#### Electron microscopy

To determine the synaptic incidence of 5-HT varicosities in the SNr and SNc, 5-HT-immunoreactive profiles were photographed at random in single ultrathin sections [from 10 rats for the SNr ( $64 \pm 28$ /rat) and from five rats for the SNc ( $42 \pm 29$ /rat)]. The area, the long and short axes and the length of synaptic contacts of the 5-HT varicosities were measured by computerized image analysis (Image 1.38; courtesy of W. Rasband, NIH) on pictures of such varicosities randomly chosen from the same material ( $n=366$  in SNr;  $n=66$  in SNc). The mean diameter and the aspect ratio were derived from the long and short axes: Mean diameter=(Long axis+Short axis)/2; Aspect ratio=Long axis/Short axis. The proportion of 5-HT axonal varicosity profiles showing a synaptic specialization in single thin sections (parallel, thickened membranes separated by an enlarged cleft filled with electron-dense material) was extrapolated to estimate the synaptic incidence of complete varicosities, using the stereological formula of Beaudet and Sotelo.<sup>3</sup> The latter calculations were performed using the long axis of the varicosity profiles, as best estimate of the diameter (or height across the sectioning plane) of whole varicosities (see Ref. 54).

To see whether TH-immunopositive or microtubule-filled, electron-dense dendrites (MT; see below) were preferred synaptic targets of the innervation by 5-HT-positive terminals, we counted the number of TH-immunolabelled, MT; and unidentified (unlabelled and not MT) dendritic profiles that were in synaptic contact with 5-HT varicosities in the SNr. The total number of TH-immunolabelled, MT; and unidentified dendritic profiles in the same sections was also counted. The following ratios were then calculated: TH-immunolabelled dendritic profiles in synaptic contact with 5-HT terminals/total number of dendritic profiles in synaptic contact with 5-HT terminals; MT dendritic profiles in synaptic contact with 5-HT terminals/total number of dendritic profiles in synaptic contact with 5-HT terminals; TH-immunolabelled dendritic profiles/total number of dendritic profiles; MT dendritic profiles/total number of dendritic profiles. To see whether 5-HT terminals made synaptic contact preferentially on larger (proximal) or smaller (distal) dendrites, the diameter (short axis) of the

dendritic profiles of each type (TH, MT or "unidentified") that were postsynaptic to 5-HT-positive varicosities was also measured using the image analysis system as well as that of all other dendritic profiles of the same types. These measurements and calculations were carried out on four rats ( $n=60 \pm 12$  profiles postsynaptic to 5-HT-positive varicosities and  $433 \pm 118$  profiles that did not have 5-HT-positive synaptic contact/rat).

#### Statistical analyses

A factorial ANOVA (Statview 4.01; Abacus Concepts, Berkeley, CA) was used to compare the number of varicosities labelled with [<sup>3</sup>H]5-HT in autoradiographs and counted in the SNr and SNc, the synaptic incidence of 5-HT-immunoreactive varicosities in the SNc and SNr, and the morphometric data on 5-HT-positive varicosity profiles that were either non-synaptic or in synaptic contact with TH-immunoreactive, MT or unidentified dendrites in the SNr. Comparison of the morphometric data on 5-HT-immunolabelled varicosities between the SNr and SNc was made using a nested ANOVA for samples of unequal sizes.<sup>47</sup> Differences in diameter between dendritic profiles that were postsynaptic to 5-HT-immunostained varicosities and those that were not were evaluated for each type of dendrite (unidentified, TH-immunopositive or MT) using a Student's *t*-test. The analysis of deviance was used to compare the synaptic incidence of 5-HT-immunolabelled varicosity profiles between the SNc and SNr and the proportions of TH-immunopositive or MT dendrites that were synaptically contacted by 5-HT-positive varicosities with the proportions of TH-immunolabelled or MT dendrites in the overall population of dendrites.<sup>30</sup> To respect the conditions of application of the ANOVA and Student's *t*-tests,<sup>47</sup> we used the square root of the area of the 5-HT-immunostained varicosity profiles, the natural logarithm of the width of their dendritic targets, and the varicosity aspect ratio was transformed into  $\sqrt{\ln(\text{aspect ratio})}$ . *A posteriori* tests were applied to locate differences between individual groups (ANOVA).

## RESULTS

#### Quantitative autoradiographic estimates of serotonin-ergic innervation

Following the uptake and storage of [<sup>3</sup>H]5-HT, light microscope autoradiographs displayed numerous silver grain aggregates, or clusters, over a background of diffuse silver grains (Fig. 1). Such silver grain clusters have previously been shown to represent labelled 5-HT axonal varicosities in the present conditions of incubation.<sup>18</sup> This selective labelling was present in all areas of the midbrain sections but was much more prominent in the substantia nigra, particularly the SNr (Fig. 1B).

In the series of autoradiographs exposed for different periods of time, the number of silver grain clusters increased with the duration of exposure, reaching a plateau around 60 days (Fig. 2). Since the background also increased with exposure time, quantification was performed on sections exposed for 21 days, which gave an optimal signal-to-noise ratio (Fig. 1C-F), and the data were extrapolated using the curve in Fig. 2A, B.<sup>17,18</sup> This analysis gave values of  $8 \times 10^3$  silver grain clusters/mm<sup>2</sup> in the SNr and  $6 \times 10^3$ /mm<sup>2</sup> in the SNc (Table 1).

These values were extrapolated to volume using the mean diameter of the 5-HT-immunoreactive

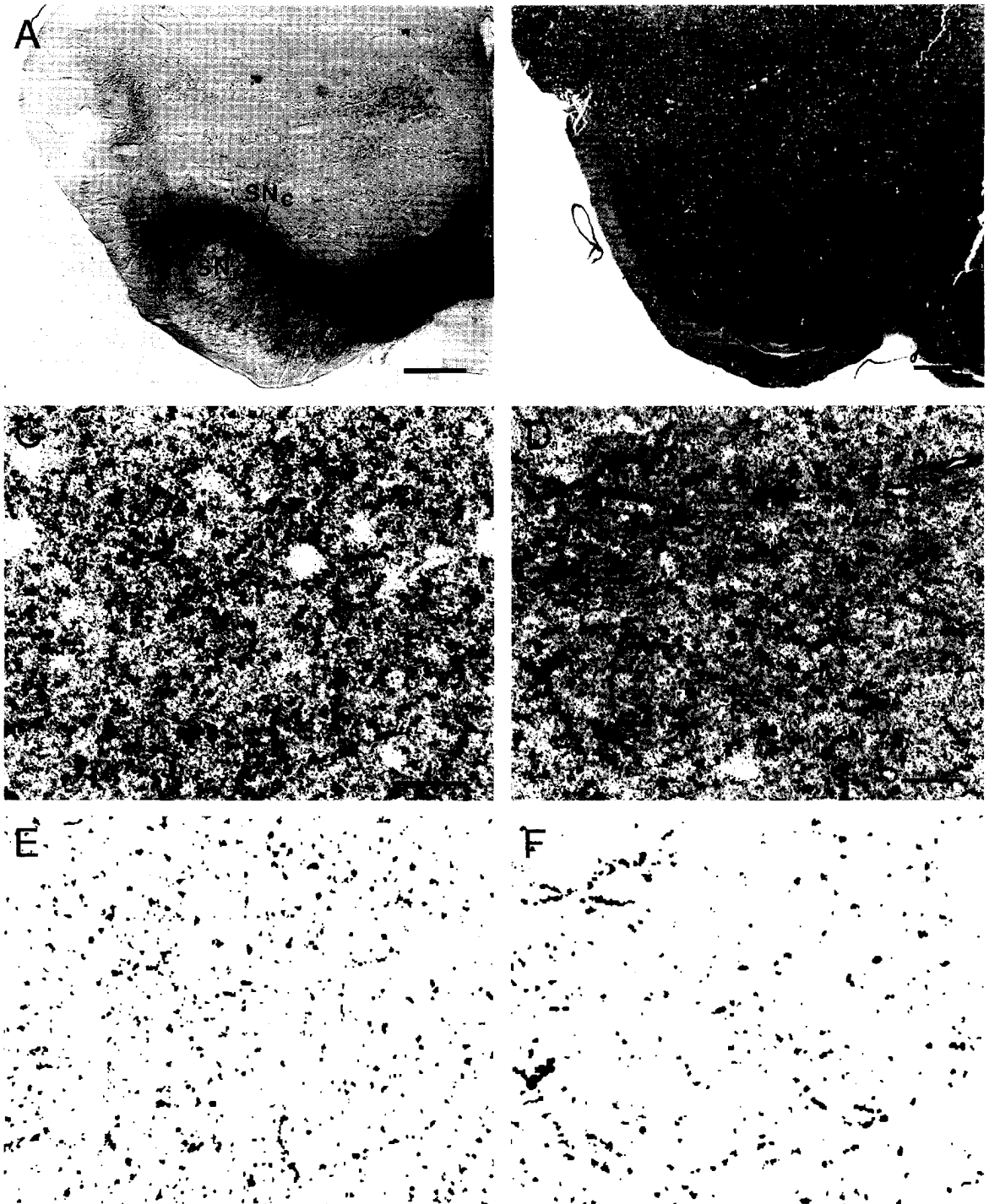


Fig. 1. Light micrographs of the rat SN. (A) Dopamine neurons visualized by TH immunostaining. The cell bodies are mostly concentrated in the SNc whereas many "apical" dendrites project into the SNr. (B) Semithin section of the SN showing 5-HT axonal varicosities revealed by autoradiography following [ $^3\text{H}$ ]5-HT uptake/storage *in vitro*. The frame represents the size of the image analysis measuring window, corresponding approximately to the area of the fields illustrated in C-F. When necessary, manual adjustments of the counting window were done in order to remain within the limits of the SNc. (C, D) 5-HT axonal varicosities visualized at higher magnification as clusters of silver grains in the SNr and SNc, respectively. (E, F) Binary images of C and D, respectively, after grey level selection of the silver grain clusters. The individual features were counted by the image analysis system. Empirically determined correction factors were used to take into account the fusion of silver grain clusters into single binary image features (see Ref. 17). Scale bars=500  $\mu\text{m}$  (A, B) and 250  $\mu\text{m}$  (C, D).

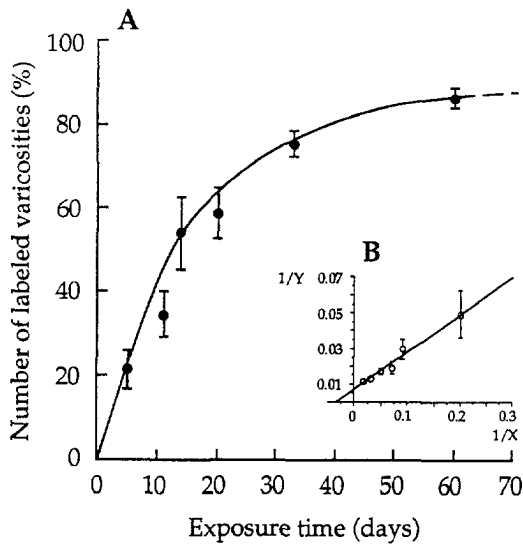


Fig. 2. (A) Number of silver grain clusters expressed as percent of the theoretical maximum and plotted against autoradiographic exposure time. Six series of semithin sections (0.5- $\mu\text{m}$ -thick) were exposed for increasing periods of time and the silver grain clusters counted in these sections were plotted. The theoretical maximum that was extrapolated from the best-fit curve (in B) was used to calculate the percentages represented in this graph. This curve was used to transform the numbers obtained after counting in autoradiographs exposed for 21 days into the numbers that would theoretically have been counted if all labelled 5-HT axonal varicosities had been detected (at the plateau). (B) The insert shows the original data plotted as double reciprocal. This curve served to estimate the theoretical maximum number of labelled terminals and calculate the percentages of the ordinate in A (see Ref. 15).

Table 1. Density of serotonin innervation in the pars reticulata and pars compacta of the substantia nigra

	SNr	SNc
Silver grain clusters $\times 10^3/\text{mm}^2$ ( $\pm$ S.D.)	$8.39 \pm 1.59$	$5.88 \pm 1.34^{***}$
5-HT varicosities $\times 10^6/\text{mm}^3$ ( $\pm$ S.D.)	$8.77 \pm 1.66$	$6.14 \pm 1.40$

Results of counts in the autoradiographs of the SNr and of the SNc after *in vitro* uptake of tritiated 5-HT, expressed as numbers of silver grain clusters/unit area, after correcting for autoradiographic exposure time, and as numbers of 5-HT varicosities/unit volume, after taking into account the diameter of the varicosities and the efficiency of detection of tritium  $\beta$  particles from sections thicker than 2  $\mu\text{m}$  (see Ref. 17). ( $^{***}P < 0.001$ , factorial ANOVA.)

varicosities, as measured by electron microscopy in the SN (Table 2), and corrected for the incomplete detection of tritium  $\beta$  particles from sections more than 2.0  $\mu\text{m}$  thick (see Refs 17 and 18). The extrapolated values were  $9 \times 10^6$  5-HT varicosities/ $\text{mm}^3$  in the SNr and  $6 \times 10^6/\text{mm}^3$  in the SNc. There was a significant difference between the values of the SNr and SNc (Table 1).

Table 2. Morphometric features of serotonin-immunoreactive axonal varicosities in the substantia nigra pars reticulata and compacta

	SNr	SNc
Number of varicosities	366	66
Area ( $\mu\text{m}^2$ )	$0.3 \pm 0.2$	$0.4 \pm 0.2$
Long axis ( $\mu\text{m}$ )	$0.8 \pm 0.3$	$0.9 \pm 0.3$
Short axis ( $\mu\text{m}$ )	$0.5 \pm 0.2$	$0.5 \pm 0.2$
Mean diameter ( $\mu\text{m}$ )	$0.6 \pm 0.2$	$0.7 \pm 0.2$
Aspect ratio	$1.7 \pm 0.6$	$1.8 \pm 0.7$

These measurements of 5-HT-immunopositive varicosities were made with an image analysis system on randomly chosen electron micrographs from single immunostained sections. (No significant difference between SNc and SNr; Nested ANOVA.)

#### Ultrastructural features of serotonin-immunoreactive varicosities in the pars reticulata and pars compacta

Light microscopic observation revealed a dense network of fine 5-HT-immunostained varicose fibres in the SN, particularly in the SNr. Varicosities of various sizes were observed on individual fibres (Fig. 3).

In the electron microscope (Fig. 4), the profiles of 5-HT-immunostained varicosities were recognized by the presence of the typical diffuse electron-dense peroxidase reaction product associated with the membranes of synaptic vesicles and mitochondria and the inner surface of the plasma membrane. Consistent with previous descriptions, they contained small clear vesicles, occasional large dense core vesicles and mitochondria.<sup>10,26,31,34,56</sup> In both SNr and SNc, the 5-HT-stained varicosities were ovoid in shape, which was reflected in the aspect ratio of 1.7. There was no significant difference in size between 5-HT-positive varicosities of these two regions (Table 2).

In most cases, the 5-HT-immunostained profiles did not show any synaptic membrane specialization when examined in single ultrathin sections (Fig. 4A, B). When present, the synapse was generally of the asymmetrical type (Figs 4D, 5B), as reported previously<sup>10</sup> (but see Ref. 31). The major difference between the two regions of the SN concerned the frequency of synaptic contacts (synaptic incidence) displayed by 5-HT-positive profiles, which was twice as great in the SNr as in the SNc (Table 3). Extrapolation to estimate the synaptic incidence for complete 5-HT varicosities showed that the large majority, if not all, were synaptic in the SNr, whereas only half were synaptic in the SNc (Table 3).

#### Synaptic targets of serotonin-immunoreactive varicosities

Serotonin-immunoreactive varicosities made synaptic contacts predominantly with dendritic shafts ranging from 0.4 to 1.6  $\mu\text{m}$  in diameter (Figs 4C, D and 6). In the SNr, 5-HT-immunostained varicosities



Fig. 3. Light micrograph of 5-HT-immunostained axons in the SNr. These fine axons bear varicosities of different sizes. Note that large and small varicosities may arise from the same axon (arrows). Scale bar=10  $\mu$ m.

Table 3. Synaptic incidence of serotonin-immunoreactive axonal varicosities in the substantia nigra pars reticulata and compacta

	SNr	SNc
Number of varicosities	593	217
Synaptic incidence in single thin sections (%)	28 $\pm$ 8	13 $\pm$ 6***
Extrapolation to whole varicosities (%)	93	49

Serotonin-immunostained axonal varicosities were photographed at random in single ultrathin sections of the SNr and SNc from 10 and six rats, respectively. The proportion of 5-HT-positive profiles showing a synaptic specialization was determined and then extrapolated to whole varicosities, according to the stereological formula of Beaudet and Sotelo,<sup>3</sup> using the long axis as an estimation of the diameter of the whole varicosities.<sup>54</sup> (\*\*\*)  $P < 0.001$ , Deviance analysis.)

made contact together with unlabelled varicosities to form "en rosette" arrangements around dendritic profiles in cross-section. The length of the synaptic contacts ranged between 0.03 and 0.75  $\mu$ m and varied depending on the target type (see below). No example of synaptic contacts by 5-HT-positive varicosities on perikarya was observed in the SNc or in the SNr.

In dual immunostained sections, the DAB reaction product for 5-HT was detected at a greater depth in the Vibratome slices than the silver-intensified immunogold labelling for TH. In ultrathin sections from the superficial region of the slices, 5-HT-immunoreactive varicosities in the SNr were frequently observed in synaptic contact with TH-immunostained dendrites (Fig. 5A, B). TH-immunolabelled dendrites represented 20  $\pm$  5% of the

structures postsynaptic to 5-HT-positive terminals, whereas they represented only 13  $\pm$  4% of the total number of dendritic profiles counted in the same sections of the SNr. The difference between these percentages was statistically significant ( $P < 0.05$ ), indicating a slight over-representation of TH-positive dendrites as postsynaptic targets of the 5-HT innervation. The diameter of the TH-immunoreactive dendritic profiles ranged from 0.45 to 2.26  $\mu$ m (mean  $\pm$  S.D. = 1.06  $\pm$  0.46  $\mu$ m). The diameter of those that were postsynaptic to 5-HT varicosities was similar, ranging from 0.34 to 2.23  $\mu$ m (1.06  $\pm$  0.57  $\mu$ m) (Fig. 6B).

Among the structures postsynaptic to 5-HT-positive terminals, TH-immunoreactive profiles had a significantly larger diameter than the unlabelled, unidentified dendritic profiles ( $P < 0.05$ ). The latter (Fig. 6A) ranged between 0.20 and 2.20  $\mu$ m (0.84  $\pm$  0.52  $\mu$ m). The unidentified dendritic profiles that were not postsynaptic to 5-HT varicosities were significantly larger than those that were postsynaptic, ranging between 0.30 and 4.30  $\mu$ m (1.54  $\pm$  0.89  $\mu$ m;  $P < 0.001$ ), indicating that 5-HT-positive varicosities preferentially contacted these dendrites in their distal regions, unless a subpopulation of unidentified neurons, with larger dendrites, is not synaptically contacted by the 5-HT innervation.

Some of the dendrites, unlabelled in TH-immunostained sections, were characterized by the presence of numerous microtubules (Fig. 4D). The cytoplasmic electron density of these dendrites (MT) ranged from clear to very dense, the one illustrated in Fig. 4D being intermediate in this respect. The contour of their cytoplasmic membrane was also often irregular. They represented 5  $\pm$  2% of the total number of dendritic profiles in the SNr and they

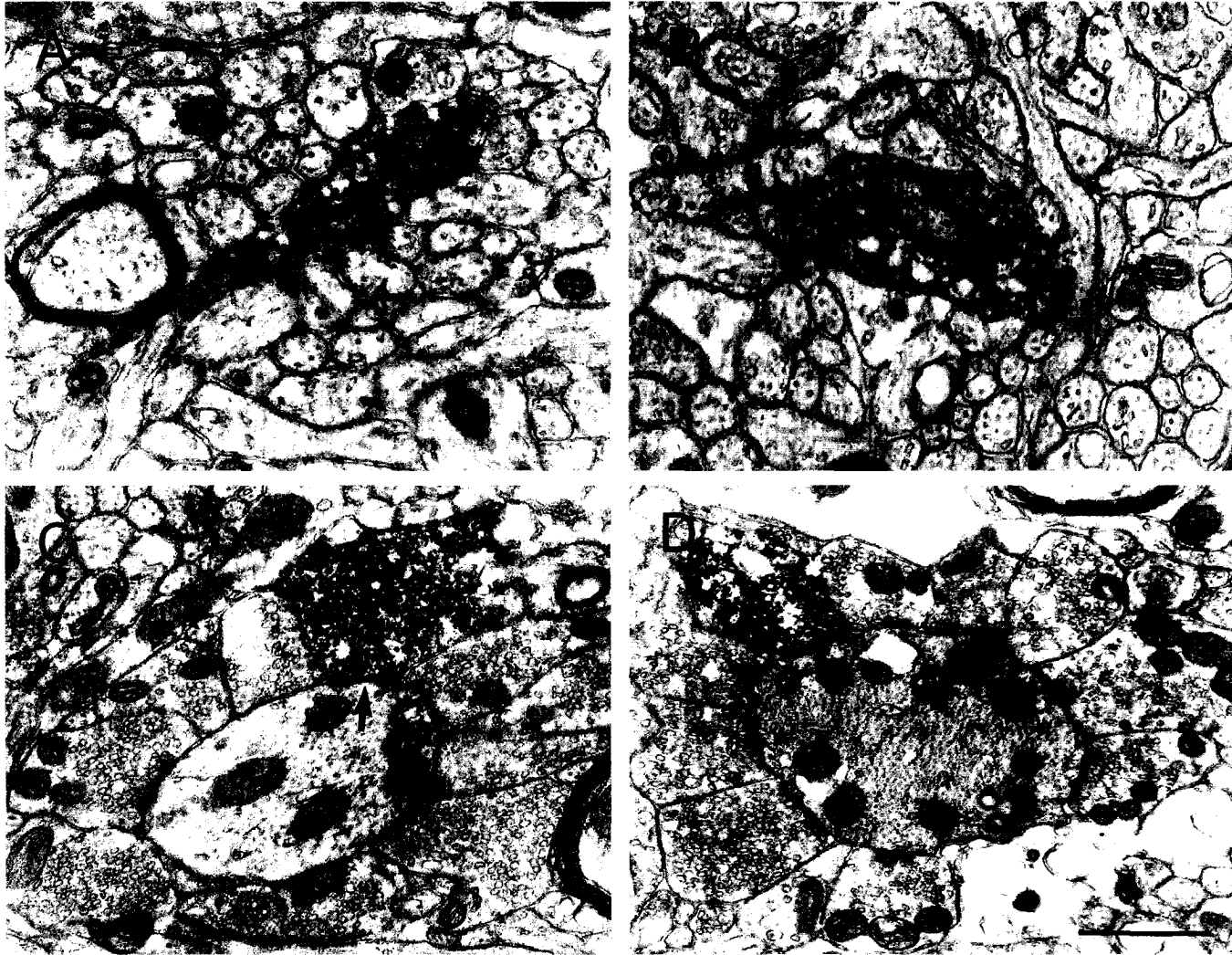


Fig. 4. Electron micrographs of 5-HT-immunoreactive axonal varicosities in the SN. (A, B) Axonal varicosities of the SNc that do not display junctional membrane specializations. Both are surrounded by unlabelled axons. (C) 5-HT-immunopositive axonal varicosity in synaptic contact with an unlabelled dendrite in the SNr. Several unlabelled terminals are also in synaptic contact with the same dendrite, forming a typical "en rosette" arrangement. (D) 5-HT-positive axonal varicosity forming an asymmetrical synaptic contact with a dendrite in the SNr characterized by a peculiarly high number of microtubules (MT), here in cross-section. Note the presence of some vacuoles and the slightly irregular contour of the cytoplasmic membrane of this profile, which also appears lightly electron-dense between the microtubules. Scale bar=0.5  $\mu$ m (A-D).

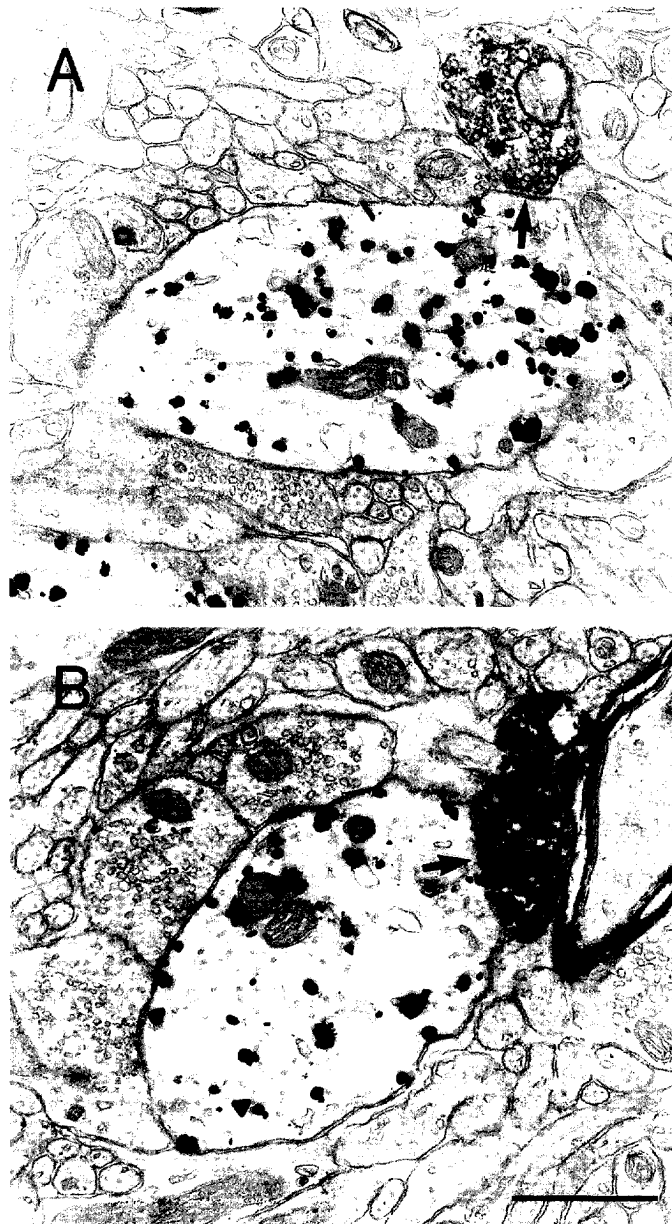


Fig. 5. (A, B) 5-HT axonal varicosities (5-HT-immunoreactive; diaminobenzidine reaction product) in synaptic contact (arrows) with dopamine dendrites (TH-immunoreactive; silver-intensified immunogold particles) following dual pre-embedding immunocytochemistry. The synapse in B is clearly asymmetrical, as was the majority of synapses formed by 5-HT-immunoreactive varicosities in the substantia nigra. Scale bar=0.5  $\mu$ m (A, B).

represented  $6 \pm 2\%$  of all postsynaptic targets of the 5-HT innervation. The diameter of the MT profiles that were postsynaptic to 5-HT-positive terminals was not statistically different from the TH-immunoreactive or the unidentified dendritic targets of 5-HT-immunoreactive axon terminals. They were, however, significantly larger than the MT dendritic profiles that were not contacted by 5-HT-positive varicosities (Fig. 6C), which suggests that the MT dendrites were preferentially innervated by 5-HT-positive terminals in their proximal portion.

#### *Morphometrics of serotonin-containing varicosities in contact with different dendritic types*

The area, diameter, aspect ratio and length of the junctional complex of the 5-HT-positive varicosity profiles that were non-synaptic or were in synaptic contact with unidentified, TH-immunoreactive or MT dendrites are shown in Table 4. Non-junctional 5-HT-positive varicosity profiles were significantly smaller than synaptic ones contacting unidentified or MT dendrites, but comparable to those contacting

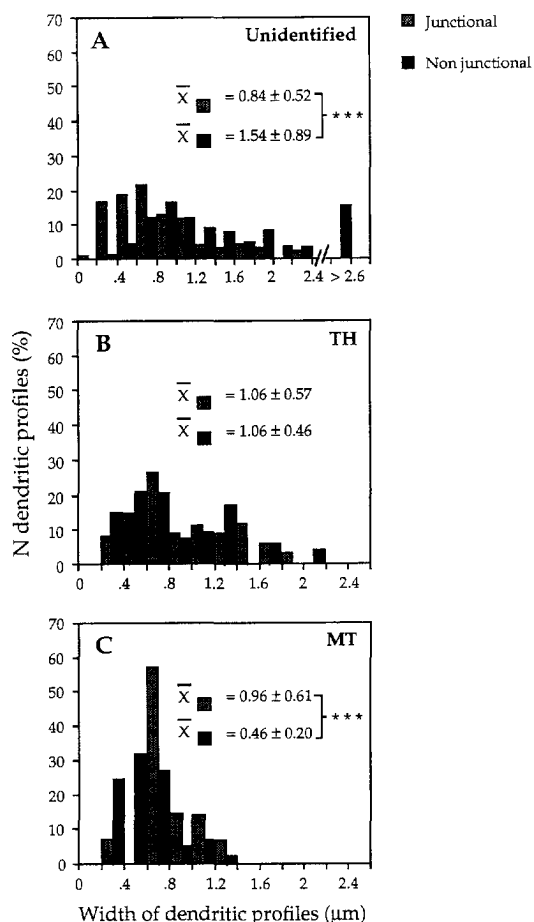


Fig. 6. Frequency distribution of the diameter of DA, MT and unidentified dendritic profiles that were postsynaptic to 5-HT-immunoreactive varicosities as opposed to those that were not associated with 5-HT-immunoreactive profiles in single sections of the SNr. A significant difference between the size of dendritic profiles which were postsynaptic to 5-HT-positive varicosities and those that were not was found for unidentified (A) and for MT dendrites (C), whereas there was no difference between DA dendrites. ( $P < 0.001$ , Student's *t*-test.)

TH-immunoreactive dendrites. The largest 5-HT-positive varicosities and junctional complexes were those contacting MT dendrites. There was a positive correlation between the size of the varicosities and the length of the synaptic junction ( $P < 0.001$ ), as described previously for unlabelled boutons contacting motoneurons in the spinal cord of the adult turtle.<sup>58</sup>

#### DISCUSSION

The results of the present study provide new information concerning the 5-HT innervation of the substantia nigra (i.e. [<sup>3</sup>H]5-HT-labelled or 5-HT-immunoreactive axonal varicosities). First, they point to the fact that both the SNc and SNr receive a dense 5-HT input and that the density of innervation is greater in the SNr than in the SNc,

exceeding that of any region of the brain so far examined. Secondly, they demonstrate that, unlike most other regions of the brain, virtually all 5-HT varicosities form synaptic specializations in the SNr, whereas only 50% do so in the SNc. Thirdly, they identify in the SNr both DA and non-DA dendrites, among which is a hitherto unidentified category characterized by a high density of microtubules, as synaptic targets for 5-HT terminals. Finally, they demonstrate that the morphometrics of 5-HT synaptic boutons in the SNr are related to their synaptic targets.

#### Density of serotonin innervation in the substantia nigra

Our quantitative results reveal that the SN receives one of the densest 5-HT projections in the brain (6–9 millions of varicosities/mm<sup>3</sup>). They are consistent with previous reports having shown that the ventral mesencephalic tegmentum including the SN contains the highest brain concentrations of endogenous 5-HT and the highest density of binding sites for high-affinity ligands of the 5-HT transporter.<sup>15,16,20,38</sup> For comparison with other basal ganglia structures, the mean density of 5-HT innervation was previously estimated to be  $4.5 \times 10^6$  varicosities/mm<sup>3</sup> in the globus pallidus,  $3 \times 10^6$ /mm<sup>3</sup> in the nucleus accumbens and  $2.6 \times 10^6$ /mm<sup>3</sup> in the neostriatum.<sup>46</sup> The density of 5-HT innervation in the normal neostriatum of adult rat was recently re-examined in the conditions used for the present experiments, which decrease background labelling resulting from low affinity uptake in DA terminals (see Ref. 17); it was estimated to be  $5.4 \times 10^6$  varicosities/mm<sup>3</sup>.<sup>48</sup>

The fact that the SNr contains a significantly higher density of 5-HT varicosities than the SNc is also in agreement with early biochemical measurements,<sup>40</sup> as well as with immunohistochemical descriptions in the rat<sup>31,49</sup> and in the monkey.<sup>29</sup> Other studies based on anterograde tracing from the dorsal raphe nucleus, however, showed that the majority of the raphe–nigral afferents innervate the SNc.<sup>2,22,57</sup> Considering the topographical organization of this projection,<sup>10</sup> these results were presumably biased by a preferential labelling of 5-HT neurons projecting to the SNc. They could also have involved a substantial number of non-5-HT neurons which represent more than two thirds of the neuronal population in the dorsal raphe nucleus.<sup>14</sup>

#### Synaptic innervation of the substantia nigra

The present electron microscopic data indicate that the 5-HT innervation is entirely synaptic in the SNr and only 50% synaptic in the SNc, where the density of innervation is also lower. It has been suggested that two morphologically distinct 5-HT fibre systems, varicose fibres and beaded fibres, innervate some forebrain regions with different synaptic incidences.<sup>51</sup>

Table 4. Morphometric features of serotonin-immunoreactive axonal varicosity profiles that were non-synaptic or contacting different dendritic targets in the substantia nigra pars reticulata

	Postsynaptic targets						
	(Non-synaptic)		TH dendrites		Unidentified dendrites		MT dendrites
Number	145		42		164		15
Area ( $\mu\text{m}^2$ )	$0.29 \pm 0.16$	$\approx$	$0.25 \pm 0.17$	<***	$0.35 \pm 0.19$	<**	$0.52 \pm 0.21$
Diameter ( $\mu\text{m}$ )	$0.61 \pm 0.18$	$\approx$	$0.55 \pm 0.20$	<***	$0.67 \pm 0.19$	<**	$0.83 \pm 0.17$
Aspect ratio	$1.7 \pm 0.6$	$\approx$	$1.7 \pm 0.5$	$\approx$	$1.7 \pm 0.6$	$\approx$	$1.6 \pm 0.3$
Junctional complex ( $\mu\text{m}$ )	-		$0.26 \pm 0.13$	$\approx$	$0.31 \pm 0.13$	<***	$0.38 \pm 0.14$

5-HT-positive varicosities and junctional complexes were measured in single thin sections of 5-HT/TH dually-immunostained Vibratome sections.  $\approx$  not statistically different, \*\* $P < 0.01$ , \*\*\* $P < 0.001$ , factorial ANOVA and Scheffé  $F$  procedure for *post hoc* comparisons.

However, in spite of a 100% synaptic incidence, we observed both small and large boutons in the SNr. Moreover, both types of boutons could even be present on the same parent axon, as observed in the light microscope. This indicates that both types of 5-HT varicosities form synaptic contacts in that part of the SN at least.

The lower synaptic incidence of 5-HT varicosities in the SNc supports the idea that 5-HT, in addition to acting at synaptic specializations, also acts at a distance by diffusion in the extracellular space, as initially proposed for 5-HT in the cerebral cortex (see Ref. 11), to reach 5-HT receptors on the DA neurons. Interestingly, a synaptic incidence of 50% has also been calculated for 5-HT terminals in the VTA,<sup>26</sup> which may represent a continuum of the dorsal SNc. In contrast, the "junctional" type of transmission appears to be the major mode of action for 5-HT in the SNr. This region comprises the GABA output neurons of the basal ganglia and the "apical" dendrites of the "inverted pyramidal" SNc DA neurons.<sup>21</sup> It remains to be established whether the 5-HT varicosities which form synaptic contacts in the SNc are aimed specifically at the "basal" dendrites of these inverted pyramidal DA neurons, or whether they are innervating as well the dendrites of the more dorsally located DA neurons of the SNc, which do not extend dendrites into the SNr.

In most other brain areas where it has been evaluated, e.g., the nucleus accumbens,<sup>56</sup> the frontoparietal cortex<sup>9,43</sup> or the hippocampus,<sup>37,53</sup> the synaptic incidence for 5-HT varicosities is lower than that observed in the SN in the present study. In the neostriatum, it is more than 10-fold lower than in the SNr.<sup>12,45</sup> Interestingly, this region receives collaterals from the majority of 5-HT neurons innervating the SN.<sup>27,55</sup> This raises the possibility that the same 5-HT neurons produce a highly synaptic innervation in one region (the SN) and a largely asynaptic innervation in another region (the striatum). However, the striatum also receives 5-HT afferents from neurons that do not project to the SN, and this issue would be better addressed by intracellular or juxtacellular injections of axonal tracers.<sup>5</sup>

### Postsynaptic targets

The postsynaptic targets of 5-HT-labelled terminals were mainly dendrites in both the SNc and the SNr, in concordance with the data of Corvaja *et al.*,<sup>10</sup> who also reported rare cases of contacts on dendritic spines. In the present study, postsynaptic elements were analysed in more detail in the SNr, which primarily contains the medium to large, aspiny, pallidal-like cell bodies of the GABAergic output neurons. Scattered medium-sized DA neurons are also present in this region, in addition to the "apical" dendrites of the inverted pyramidal DA neurons from the SNc.<sup>21</sup> We distinguished at least three types of dendritic targets of the 5-HT innervation: TH-immunoreactive (DA) dendrites, which appeared to be somewhat over-represented and could therefore constitute preferential targets, unlabelled dendrites characterized by a high content of microtubules (MT) and unlabelled, non-identified dendrites that could belong to more than one neuronal type. The fact that these three types of dendrites exhibited different morphometric features indicates that they probably belong to different neuronal populations, while confirming that DA neurons are not the sole synaptic targets of the 5-HT innervation in the SN.<sup>10</sup> This provides an anatomical substrate for the *in vivo* locomotor effects of locally applied 5-HT agonists after destruction of DA neurons with 6-hydroxydopamine.<sup>36</sup> Among non-DA targets, GABAergic output neurons are good candidates since 5-HT was reported to have an excitatory action, via 5-HT<sub>2C</sub> receptors, on SNr neurons.<sup>42</sup>

The MT dendrites, whose high content in microtubules would reflect a peculiar cytoskeleton organization, have not been described previously. Preliminary observations following post-embedding immunocytochemistry suggest that they may be GABAergic (unpublished observations), but whether they belong to projection neurons and/or to interneurons remains to be determined. The electron density and irregular contour of the membrane of some of these profiles suggest that they might represent so-called "dark neurons",<sup>6</sup> an artifact produced

by *post mortem* traumatization of nervous tissue.<sup>7</sup> The presence of a few dark neurons was indeed confirmed in Methylene Blue-stained semithin sections of the same material. Such neurons were found exclusively in the SN (with rare cases in globus pallidus), as well as MT dendritic profiles. However, previous reports on the ultrastructure of dark cells in other regions of the brain never mentioned the presence of increased numbers of microtubules in such neurons (e.g., Ref. 50). The fact that the MT dendrites also showed special relationships with 5-HT varicosities (see below) is strongly in favour of the hypothesis that they belong to a separate population of neurons that might be particularly sensitive to *post mortem* traumatic artifacts.

In order to determine whether the synaptic 5-HT varicosities preferentially contacted dendrites of larger or smaller size, we compared the diameter of the dendritic profiles that were synaptically contacted by 5-HT-immunostained varicosities to that of all other dendritic profiles of the same type (TH, MT or "unidentified"). From these quantitative data we conclude that 5-HT afferents contact their different neuronal targets on different proximodistal portions of their dendritic trees. Indeed, the absence of a difference in mean diameter or size distribution for TH-immunopositive dendritic profiles that were postsynaptic and those that were not indicates that the 5-HT input is uniformly distributed along DA dendrites. In contrast, 5-HT varicosities appear to contact "unidentified" dendrites more distally, since the profiles of these dendrites were generally smaller when synaptically contacted, whereas they apparently contact MT dendrites more proximally, since the profiles of MT dendrites were generally larger when seen in synaptic contact with a 5-HT-immunoreactive varicosity. Therefore, not only is the 5-HT input to the SNr entirely synaptic and selectively targeting dendrites, but it is also imparted with specific portions of some dendrites.

It will be interesting to see whether the differences in 5-HT innervation between the SNr and SNc, as well as among synaptic targets in the SNr, reflect differential distributions of nigral 5-HT receptors, which are largely confined to the SNr, where the 5-HT<sub>1B</sub>, 2A, 2B and 4 subtypes are present (references in Ref. 42).

#### *Retrograde influence of the targets on serotonergic varicosities?*

The size of the 5-HT varicosities differed depending on the nature of the postsynaptic dendrite. Since

varicosities of different sizes were present on the same parent 5-HT axons, this observation raises the possibility that the size of the 5-HT varicosities could be partly dependent on local interactions with their postsynaptic targets. A retrograde effect of the target region as a whole on the size of afferent terminals has indeed been reported by Zwimpfer *et al.*,<sup>59</sup> following experiments with peripheral nerve transplants inducing ectopic growth of optic nerve axons into the cerebellum; the authors suggested a role for neurotrophins in these effects. Infusions of nerve growth factor have also been demonstrated to induce a hypertrophy of cholinergic terminals in the lesioned cerebral cortex.<sup>24</sup>

### CONCLUSIONS

Serotonin neurons are generally viewed as neurons with diffuse and widespread projections bearing few synaptic specializations<sup>13,44,51</sup> and therefore involved mainly in a mode of communication also referred to as "volume transmission", as opposed to "wiring transmission".<sup>1,23</sup> The present data indicate that both "non-junctional" and "junctional" transmission occur in the SNc, whereas the predominant mode of transmission in the SNr is apparently of the "junctional" type. Considering the high density of the nigral 5-HT input, the point-to-point cellular interrelationships established by this input in the SNr should constitute one important link in the neuronal circuitry subserving the role of the SN in the control of motor functions. The fact that the 5-HT fibres in the SNr, which also receives a topographically-organized projection from the neostriatal matrix (see Ref. 21), are in a situation not only to directly excite the GABA output neurons, but also to precisely control the dendritic release of DA in their micro-environment, appears of significant value in this respect.

*Acknowledgements*—The authors thank Mr G. Lambert for his photographic work and Dr A. Mrini for his help in image analysis. We also thank Dr V. Pickel for demonstration of immunogold labelling in her laboratory. This study was supported by the Canadian and the British Medical Research Councils (MRC), by the Fonds de la Recherche en Santé du Québec (FRSQ), the Banting Research Foundation and the Université de Montréal (CAFIR). G.D. was supported by a scholarship from the FRSQ, H.M. by fellowships from the Groupe de recherche sur le système nerveux central (FCAR grant) and the Canadian MRC, and O.B. by a travel grant from the French CNRS/Canadian MRC exchange program.

### REFERENCES

1. Agnati L. F., Zoli M., Strömberg I. and Fuxe K. (1995) Intercellular communication in the brain: wiring versus volume transmission. *Neuroscience* **69**, 711–726.
2. Azmitia E. C. and Segal M. (1978) An autoradiographic analysis of the differential ascending projections of the dorsal and median raphe nuclei in the rat. *J. comp. Neurol.* **179**, 641–668.

3. Beaudet A. and Sotelo C. (1981) Synaptic remodeling of serotonin axon terminals in rat agranular cerebellum. *Brain Res.* **206**, 305–329.
4. Blackburn T. P., Cox B., Heapy C. G., Lee T. F. and Middlemiss D. N. (1981) Supersensitivity of nigral serotonin receptors and rat rotational behaviour. *Eur. J. Pharmac.* **71**, 343–346.
5. Bourassa J., Pinault D. and Deschenes M. (1995) Corticothalamic projections from the cortical barrel field to the somatosensory thalamus in rats — a single-fibre study using biocytin as an anterograde tracer. *Eur. J. Neurosci.* **7**, 19–30.
6. Brown A. W. (1977) Structural abnormalities in neurones. *J. clin. Path.* **30**, 155–169.
7. Cammermeyer J. (1961) The importance of avoiding “dark” neurons in experimental neuropathology. *Acta neuropath.* **1**, 245–270.
8. Chan J., Aoki C. and Pickel V. M. (1990) Optimization of differential immunogold–silver and peroxidase labeling with maintenance of ultrastructure in brain sections before plastic embedding. *J. Neurosci. Meth.* **33**, 113–127.
9. Cohen Z., Ehret M., Maitre M. and Hamel E. (1995) Ultrastructural analysis of tryptophan hydroxylase immunoreactive nerve terminals in the rat cerebral cortex and hippocampus: their association with local blood vessels. *Neuroscience* **66**, 555–569.
10. Corvaja M., Doucet G. and Bolam J. P. (1993) Ultrastructure and synaptic targets of the raphe–nigral projection in the rat. *Neuroscience* **55**, 417–427.
11. Descarries L., Séguéla P. and Watkins K. C. (1991) Nonjunctional relationships of monoamine axon terminals in the cerebral cortex of adult rat. In *Volume Transmission in the Brain: Novel Mechanisms for Neural Transmission* (eds Fuxe K. and Agnati L. F.), pp. 53–62. Raven Press, New York.
12. Descarries L., Soghomonian J.-J., Garcia S., Doucet G. and Bruno J. P. (1992) Ultrastructural analysis of the serotonin hyperinnervation in adult rat neostriatum following neonatal dopamine denervation with 6-hydroxydopamine. *Brain Res.* **569**, 1–13.
13. Descarries L. and Umbriaco D. (1995) Ultrastructural basis of monoamine and acetylcholine function in CNS. *Semin. Neurosci.* **7**, 309–318.
14. Descarries L., Watkins K. C., Garcia S. and Beaudet A. (1982) The serotonin neurons in nucleus raphe dorsalis of adult rat: a light and electron microscope radioautographic study. *J. comp. Neurol.* **207**, 239–254.
15. Dewar K. M., Grondin L., Carli M., Lima L. and Reader T. A. (1992) [<sup>3</sup>H]Paroxetine binding and serotonin content of rat cortical areas, hippocampus, neostriatum, ventral mesencephalic tegmentum, and midbrain raphe nuclei region following *para*-chlorophenylalanine and *para*-chloroamphetamine treatment. *J. Neurochem.* **58**, 250–257.
16. Dewar K. M., Reader T. A., Grondin L. and Descarries L. (1991) [<sup>3</sup>H]Paroxetine binding and serotonin content of rat and rabbit cortical areas, hippocampus, neostriatum, ventral mesencephalic tegmentum, and midbrain raphe nuclei region. *Synapse* **9**, 14–26.
17. Doucet G. and Descarries L. (1993) Quantification of monoamine innervations by light microscopic autoradiography following tritiated monoamine uptake in brain slices. *Neurosci. Protocols* 93-050-09-01-15.
18. Doucet G., Descarries L., Audet M. A., Garcia S. and Berger B. (1988) Radioautographic method for quantifying regional monoamine innervations in the rat brain: application to the cerebral cortex. *Brain Res.* **441**, 233–259.
19. Doucet G., Murata Y., Brundin P., Bosler O., Mons N., Geffard M., Ouimet C. C. and Björklund A. (1989) Host afferents into intrastriatal transplants of fetal ventral mesencephalon. *Expl Neurol.* **106**, 1–19.
20. Duncan G. E., Little K. Y., Kirkman J. A., Kaldas R. S., Stumpf W. E. and Breese G. R. (1992) Autoradiographic characterization of <H-3>imipramine and <H-3>citalopram binding in rat and human brain — species differences and relationships to serotonin innervation patterns. *Brain Res.* **591**, 181–197.
21. Fallon J. H. and Loughlin S. E. (1995) Substantia nigra. In *The Rat Nervous System* (ed. Paxinos G.), p. 1136. Academic Press, San Diego.
22. Fibiger H. C. and Miller J. J. (1977) An anatomical and electrophysiological investigation of the serotonergic projection from the dorsal raphe nucleus to the substantia nigra in the rat. *Neuroscience* **2**, 975–987.
23. Fuxe K. and Agnati L. F. (1991) Two principal modes of electrochemical communication in the brain: volume versus wiring transmission. In *Volume Transmission in the Brain: Novel Mechanisms for Neural Transmission* (eds Fuxe K. and Agnati L. F.), pp. 1–9. Raven Press, New York.
24. Garofalo L., Ribeiro dasilva A. and Cuervo A. C. (1992) Nerve growth factor-induced synaptogenesis and hypertrophy of cortical cholinergic terminals. *Proc. natn. Acad. Sci. U.S.A.* **89**, 2639–2643.
25. Geffard M., Tuffet S. and Peuble L. and Patel S. (1988) Production of antisera to serotonin and their metabolites and their use in immunocytochemistry. In *Neuronal Serotonin* (eds Osborne N. N. and Hamon M.), pp. 1–23. Wiley, London.
26. Hervé D., Pickel V. M., Joh T. H. and Beaudet A. (1987) Serotonin axon terminals in the ventral tegmental area of the rat: fine structure and synaptic input to dopaminergic neurons. *Brain Res.* **435**, 71–83.
27. Imai H., Steindler D. A. and Kitai S. T. (1986) The organization of divergent axonal projections from the midbrain raphe nuclei in the rat. *J. comp. Neurol.* **243**, 363–380.
28. Jacobs B. L. and Fornal C. A. (1993) 5-HT and motor control — a hypothesis. *Trends Neurosci.* **16**, 346–352.
29. Lavoie B. and Parent A. (1990) Immunohistochemical study of the serotonergic innervation of the basal ganglia in the squirrel monkey. *J. comp. Neurol.* **299**, 1–16.
30. McPherson G. (1990) *Statistics in Scientific Investigation. Its Basis, Application and Interpretation*. Springer-Verlag, New York.
31. Mori S., Matsuura T., Takino T. and Sano Y. (1987) Light and electron microscopic immunohistochemical studies of serotonin nerve fibers in the substantia nigra of the rat, cat and monkey. *Anat. Embryol.* **176**, 13–18.
32. Mounir A., Chkirate M., Vallée A., Pierret P., Geffard M. and Doucet G. (1994) Host serotonin axons innervate intrastriatal ventral mesencephalic grafts after implantation in newborn rat. *Eur. J. Neurosci.* **6**, 1307–1315.
33. Mrini A., Moukhles H., Bosler O., Jacomy H. and Doucet G. (1995) Efficient immunodetection of protein antigens in glutaraldehyde-fixed brain tissue. *J. Histochem. Cytochem.* **43**, 1285–1291.
34. Nedergaard S., Bolam J. P. and Greenfield S. A. (1988) Facilitation of a dendritic calcium conductance by 5-hydroxytryptamine in the substantia nigra. *Nature* **333**, 174–177.
35. Nedergaard S., Flatman J. A. and Engberg I. (1991) Excitation of substantia nigra pars compacta neurones by 5-hydroxy-tryptamine *in vitro*. *NeuroReport* **2**, 329–332.

36. Oberlander C., Hunt P. F., Dumont C. and Boisser J. R. (1981) Dopamine independent rotational response to unilateral intra-nigral injection of serotonin. *Life Sci.* **28**, 2595–2601.
37. Oleskevich S., Descarries L., Watkins K. C., Seguela P. and Daszuta A. (1991) Ultrastructural features of the serotonin innervation in adult rat hippocampus — an immunocytochemical description in single and serial thin sections. *Neuroscience* **42**, 777–791.
38. Palkovits M., Brownstein M. and Saavedra J. M. (1974) Serotonin content of the brain stem nuclei in the rat. *Brain Res.* **80**, 237–249.
39. Paxinos G. and Watson C. (1986) *The Rat Brain in Stereotaxic Coordinates*. Academic Press, Sydney.
40. Reubi J.-C. and Emson P. C. (1978) Release and distribution of endogenous 5-HT in the rat substantia nigra. *Brain Res.* **139**, 164–168.
41. Reynolds E. S. (1963) The use of lead citrate at high pH as an electron opaque stain in electron microscopy. *J. Cell Biol.* **17**, 208–212.
42. Rick C. E., Stanford I. M. and Lacey M. G. (1995) Excitation of rat substantia nigra pars reticulata neurons by 5-hydroxytryptamine *in vitro*: evidence for a direct action mediated by 5-hydroxytryptamine<sub>2C</sub> receptors. *Neuroscience* **69**, 903–913.
43. Séguéla P., Watkins K. C. and Descarries L. (1989) Ultrastructural relationships of serotonin axon terminals in the cerebral cortex of the adult rat. *J. comp. Neurol.* **289**, 129–142.
44. Soghomonian J.-J. and Beaudet A. and Descarries L. (1988) Ultrastructural features of central serotonin neurons. In *Neuronal Serotonin* (eds Osborne N. N. and Hamon M.), pp. 57–92. Wiley, London.
45. Soghomonian J.-J., Descarries L. and Watkins K. C. (1989) Serotonin innervation in adult rat neostriatum. II. Ultrastructural features: a radioautographic and immunocytochemical study. *Brain Res.* **481**, 67–86.
46. Soghomonian J.-J., Doucet G. and Descarries L. (1987) Serotonin innervation in adult rat neostriatum. I. Quantified regional distribution. *Brain Res.* **425**, 85–100.
47. Sokal R. R. and Rohlf F. J. (1995) *Biometry. The Principles and Practice of Statistics in Biological Research*. W. H. Freeman and Co., San Francisco.
48. Soucy J.-P., Lafaille F., Lemoine P., Mrini A. and Descarries L. (1994) Validation of the transporter ligand cyanoimipramine as a marker of serotonin innervation density in brain. *J. Nucl. Med.* **35**, 1822–1830.
49. Steinbusch H. W. M. (1981) Distribution of serotonin-immunoreactivity in the central nervous system of the rat. Cell bodies and terminals. *Neuroscience* **6**, 557–618.
50. Stensaas S. S., Edwards C. Q. and Stensaas L. J. (1972) An experimental study of hyperchromic nerve cells in the cerebral cortex. *Expl Neurol.* **36**, 472–487.
51. Törk I. (1990) Anatomy of the serotonergic system. In *The Neuropharmacology of Serotonin* (eds Whitaker-Azmitia P. M. and Peroutka S. J.), pp. 9–35. The New York Academy of Sciences, New York.
52. Trent F. and Tepper J. M. (1991) Dorsal raphe stimulation modifies striatal-evoked antidromic invasion of nigral dopaminergic neurons *in vivo*. *Expl Brain Res.* **84**, 620–630.
53. Umbriaco D., Garcia S., Beaulieu C. and Descarries L. (1995) Relational features of acetylcholine, noradrenaline, serotonin and GABA axon terminals in the stratum radiatum of adult rat hippocampus (CA1). *Hippocampus* **5**, 605–620.
54. Umbriaco D., Watkins K. C., Descarries L., Cozzari C. and Hartman B. K. (1994) Ultrastructural and morphometric features of the acetylcholine innervation in adult rat parietal cortex. An electron microscopic study in serial sections. *J. comp. Neurol.* **348**, 351–373.
55. van der Kooy D. and Hattori T. (1980) Dorsal raphe cells with collateral projections to the caudate–putamen and substantia nigra: a fluorescent retrograde double study in the rat. *Brain Res.* **186**, 1–7.
56. Vanbockstaele E. J. and Pickel V. M. (1993) Ultrastructure of serotonin-immunoreactive terminals in the core and shell of the rat nucleus accumbens — cellular substrates for interactions with catecholamine afferents. *J. comp. Neurol.* **334**, 603–617.
57. Vertes R. P. (1991) A PHA-L analysis of ascending projections of the dorsal raphe nucleus in the rat. *J. comp. Neurol.* **313**, 643–668.
58. Yeow M. B. L. and Peterson E. H. (1991) Active zone organization and vesicle content scale with bouton size at a vertebrate central synapse. *J. comp. Neurol.* **307**, 475–486.
59. Zwimpfer T. J., Aguayo A. J. and Bray G. M. (1992) Synapse formation and preferential distribution in the granule cell layer by regenerating retinal ganglion cell axons guided to the cerebellum of adult hamsters. *J. Neurosci.* **12**, 1144–1159.

(Accepted 1 August 1996)